Spatial eigenmodes of light in atmospheric turbulence

Vyacheslav Shatokhin, David Bachmann, Giacomo Sorelli, Nicolas Treps, Andreas Buchleitner

Spatial eigenmodes of light in atmospheric turbulence

Vyacheslav Shatokhin[1,2], David Bachmann[1], Giacomo Sorelli[3,4,5], Nicolas Treps[3], Andreas Buchleitner[1,2]

[1] Physikalisches Institut, Albert-Ludwigs-Universität Freiburg, Hermann-Herder-Str. 3, D-79104 Freiburg, Germany

[2] EUCOR Centre for Quantum Science and Quantum Computing, Albert-Ludwigs-Universität Freiburg, Hermann-Herder-Str. 3, 79104 Freiburg, Germany

[3] Laboratoire Kastler Brossel, Sorbonne Université, ENS-Université PSL, Collège de France, CNRS; 4 place Jussieu, F-75252 Paris, France

[4] DEMR, ONERA, Université Paris Saclay, F-91123, Palaiseau, France

[5] Sorbonne Université, CNRS, LIP6, 4 place Jussieu, F-75005 Paris, France

ABSTRACT

We carry out a numerical analysis of the spatial structure of the eigenmodes of light in atmospheric turbulence and assess the distribution of the singular values under variable turbulence conditions characterized by the Fried parameter and Rytov variance. Under weak scintillation, the highly transmitting eigenmodes found here possess a modal structure that is reminiscent of Laguerre-Gaussian (LG) modes and their simple superpositions. When scintillation becomes significant, we establish that the optimal eigenmodes for communication differ substantially from LG modes and tend to have highly localized transverse intensity distributions.

1. INTRODUCTION

Photons are standard information carriers in free-space quantum communication.[1] Until recently, mostly their polarization degree of freedom has been used to encode information into qubits.[2,3] However, photons also offer higher dimensional, spatial degrees of freedom, which allow for qu*d*it encoding in d-dimensional Hilbert spaces.[4] This promises increased channel capacities, enhanced security of quantum key distribution (QKD),[5] and stronger violations of Bell-type inequalities.[6]

There are two, apparently very different, approaches to high-dimensional spatial encoding. One is based on using fixed sets of modes. The most common example of the latter is Laguerre-Gaussian (LG) beams,[7] which carry an orbital-angular momentum (OAM) and form a complete, orthonormal, and unbounded basis.[8] Alternative sets include Bessel-Gaussian (BG),[9] as well as Hermite-Gaussian (HG)[10] and Ince-Gaussian (IG)[11] beams.

The main advantage of using fixed modes is that the latter can be generated and detected using fast and compact passive devices.[12] However, pre-determined sets of modes are not designed for the propagation through atmospheric turbulence, which causes beam wandering, phase and intensity fluctuations, and other disturbances of the propagated modes.[13] These perturbations amount to turbulence-induced losses and crosstalk among spatial modes[14] and can potentially obliterate quantum communication.[15,16] Although partial mitigation of turbulence effects is possible, e.g., by employing modal diversity,[17] entanglement concentration,[18] adaptive optics[19,20] or compressed sensing,[21] overcoming atmospheric effects still remains the greatest challenge towards long-distance free-space quantum communication based on high-dimensional spatial encoding.

On the contrary, within the second approach to spatial encoding, which we pursue in our present work, quantum information is encoded not into fixed modes but rather into spatial eigenmodes* of light for a given

Send correspondence to vyacheslav.shatokhin@physik.uni-freiburg.de

*Throughout this work, for the sake of brevity we oftentimes use the terms *eigenmodes* and *eigenvalues* somewhat loosely – to refer to highly transmitting, or optimal, spatial modes of light for a given realization of turbulence. A strict mathematical definition of such modes and their singular values, which are actually obtained from the singular value decomposition of the transmission matrix of a turbulence channel, is presented in section 2.5.

realization of turbulence ("frozen" atmosphere). By construction, such eigenmodes are mutually orthogonal and can be used for spatial encoding of high-dimensional quantum states. Furthermore, since the associated eigenvalues determine the actual transmission fidelities, eigenmodes with large eigenvalues can be transmitted through the atmosphere with little loss and distortion.[22]

While the 'eigenmodes' approach has been intensively used for transmission of information and imaging in strongly scattering media,[23] its application to free-space communication has been relatively rare.[24–26] Under weak scintillation, an eigenmode decomposition corresponding to a turbulence medium confined between the input and output circular apertures was for the first time considered by J.H. Shapiro,[24] who used asymptotic methods to establish the close similarity between significant eigenmodes (that is, those with associated eigenvalues close to one) and prolate spheroidal wavefunctions.[27] The eigenmodes encoding in the limit of weak scintillation was recently revisited,[25] and it was analytically shown that prolate spheroidal wavefunctions behave like scaled LG functions. Furthermore, some authors claimed[26] that even in strong turbulence eigenmodes of light are well-approximated by LG beams. If true, these results[25,26] would link the two aforementioned approaches to high-dimensional spatial encoding and open up exciting prospectives for robust and lossless free-space communication under arbitrary turbulence conditions employing the well-known family of LG modes.

The previous results on the atmospheric eigenmodes of light in turbulence[24–26] were obtained using approximate analytical methods with restricted validity range. Therefore, in our present contribution, we re-examine the fundamental properties of the eigenmodes in a "frozen" atmosphere numerically using multiple phase screen method,[28–30] which allows one to attain accurate modelling of a turbulence channel for a broad range of turbulence conditions.[14,19,31] In qualitative agreement with previous findings,[24,25] we obtain that under weak scintillation the eigenmodes of turbulence are similar to LG modes and their simple superpositions characterized by lobed intensity distributions. However, when scintillation becomes significant, we find that highly transmitting eigenmodes of turbulence are not LG beams but spatial modes with a highly localized transverse intensity distribution.

2. ATMOSPHERIC TURBULENCE

2.1 Stochastic parabolic equation

We find optical eigenmodes in atmospheric turbulence from the singular-value decomposition (SVD)[23,32] of a transmission matrix, which represents, in a specific basis, the turbulence operator. The latter emerges from a numerical solution of the stochastic parabolic equation[13]

$$2ik\frac{\partial u(\mathbf{r})}{\partial z} + \Delta_\perp u(\mathbf{r}) + 2k^2 n_1(\mathbf{r})u(\mathbf{r}) = 0, \tag{1}$$

where k is the signal wave number, $\Delta_\perp$ the transversal part of the Laplace operator, z the propagation direction, and $n_1(\mathbf{r})$ the fluctuating part of the refractive index of air. We note that $n_1(\mathbf{r})$ in (1) is time-independent, implying a "frozen" atmosphere, which is adequate since light propagation is much faster than the time scale of ~ 10 ms on which the atmosphere changes its state.[33]

Turbulence enters (1) via the statistical properties of $n_1(\mathbf{r})$. The refractive index fluctuations are assumed to be a zero-mean, homogeneous, Gaussian random field, whose two-point correlation function, in Markov approximation[34] along the propagation direction, is given by[13] $\langle n_1(\mathbf{r}_1)n_1(\mathbf{r}_2)\rangle = \delta(z_1 - z_2)A_n(\boldsymbol{\rho}_1 - \boldsymbol{\rho}_2)$, with $\mathbf{r} = (\boldsymbol{\rho}, z)$, and A_n the two-dimensional covariance in the transverse plane. Starting from Kolmogorov's theory of turbulence,[35] the covariance function is obtained as the Fourier transform of the refractive-index *power spectral density* $\Phi_n(\boldsymbol{\kappa})$. In the inertial range, that is, for spatial wave numbers $|\boldsymbol{\kappa}|$ satisfying the inequality $L_0^{-1} \ll |\boldsymbol{\kappa}| \ll l_0^{-1}$, where L_0 and l_0 are the outer and inner scales of turbulence, respectively (typically, $L_0 \sim 10 - 100$ m and $l_0 \sim 1 - 10$ mm[13]), $\Phi_n(\boldsymbol{\kappa}) = 0.033C_n^2\kappa^{-11/3}$, with C_n^2 the refractive index structure constant, and $\kappa := |\boldsymbol{\kappa}|$. Furthermore, turbulence is assumed to be isotropic, i.e. $A_n(\boldsymbol{\rho}_1 - \boldsymbol{\rho}_2) = A_n(|\boldsymbol{\rho}_1 - \boldsymbol{\rho}_2|)$.

2.2 Propagation regimes

Optical turbulence can be characterized by two qualitatively different propagation regimes – of weak and strong scintillation[13] – distinguished by the value of the *Rytov variance* $\sigma_R^2 = 1.23 C_n^2 k^{7/6} z^{11/6}$: scintillation is weak if $\sigma_R^2 < 1$, and strong otherwise. In the optical frequency domain, the strong scintillation regime emerges for propagation distances exceeding few kilometers.[33] Until then, the turbulence effects on the propagating wave can be oftentimes reduced to random phase errors, which can be described within the single phase screen model of turbulence.[13] A phase screen is fully characterized by the *transverse coherence length*, which is the distance over which turbulence-induced phase distortions are correlated, also known as the *Fried parameter* $r_0 = (0.423 k^2 C_n^2 z)^{-3/5}$.[13] For a given r_0, the statistics of the phase errors is described by the *phase structure function* $\langle [\phi(\boldsymbol{\rho}_1) - \phi(\boldsymbol{\rho}_2)]^2 \rangle =: D_\phi(|\boldsymbol{\rho}_1 - \boldsymbol{\rho}_2|) = 6.88 (|\boldsymbol{\rho}_1 - \boldsymbol{\rho}_2|/r_0)^{5/3}$. With the help of r_0, the turbulence strength experienced by an optical beam of diameter w_0 is defined as the ratio $W = w_0/r_0$.[13]

A single phase screen model[13] allows for an analytical[36] or numerical account of turbulence effects on short free-space links. A numerical treatment has the decisive advantage of being systematically generalizable to the strong scintillation regime,[28] wherein an extended atmospheric layer is modelled by a sequence of random phase screens introducing phase errors. In between the screens the wave experiences free diffraction in vacuum. In other words, a multiple phase screen (MPS) model represents a split-step method to solve (1). The algorithms for generating individual phase screens are well-known,[28–30] whereas their number along the light path is determined by a simple criterion: For each elementary propagation step of two vacuum propagations connected by one phase screen, scintillation must be weak (in our simulation we required even more stringently $\sigma_R^2 < 0.5$). In this work, we address weak, moderate, and strong scintillation conditions, with maximum $\sigma_R^2 = 6.31$, for which modelling we employ the MPS model of turbulence.

2.3 Turbulence operator

We introduce the *turbulence operator* $T(\boldsymbol{\rho}, \Delta z)$ when solving (1) numerically by the split-step method. On an interval Δz between the planes z_l and z_{l+1}, for which scintillation is weak (see Sec. 2), the solution of (1) can be expressed as[37] $u(\boldsymbol{\rho}, z_{l+1}) = T(\boldsymbol{\rho}, \Delta z)\, u(\boldsymbol{\rho}, z_l)$, where the turbulence operator reads

$$T(\boldsymbol{\rho}, \Delta z) = D\left(\frac{\Delta z}{2}\right) R(\boldsymbol{\rho}, z_l, z_{l+1})\, D\left(\frac{\Delta z}{2}\right), \tag{2}$$

with

$$D(z) = \exp\left(-i \frac{z}{2k} \Delta_\perp\right), \tag{3}$$

and

$$\begin{aligned} R(\boldsymbol{\rho}, z_l, z_{l+1}) &= \exp\left(-ik \int_{z_l}^{z_{l+1}} n_1(\boldsymbol{\rho}, z) dz\right) \\ &= \exp\{-i\varphi(\boldsymbol{\rho})\}, \end{aligned} \tag{4}$$

describing, respectively, diffraction and refraction on a thin turbulent layer (i.e. a phase screen). For arbitrary L, we split the path into N sufficiently small intervals, on each of which we can represent the solution in the above operator form, to obtain $u(\boldsymbol{\rho}, L) = T(\boldsymbol{\rho}, L)\, u(\boldsymbol{\rho}, 0)$, where

$$T(\boldsymbol{\rho}, L) = T(\boldsymbol{\rho}, \Delta z_1) \ldots T(\boldsymbol{\rho}, \Delta z_N). \tag{5}$$

In the weak scintillation limit, we employ a single phase screen model of turbulence, with $T(\boldsymbol{\rho}, L)$ given by (2); in the cases of moderate and strong scintillation, the turbulence operator is given by the multiple phase screen model (5), with N determined by a given value of the Rytov variance σ_R^2 (see Sec. 2.2). We generate phase screens using the subharmonics method,[30,38,39] which allows for a precise emulation of the statistics of phase errors for a broad range of spatial frequencies by variable grid spacing.

The turbulence maps (2), and consequently (5), generate unitary evolutions,[19] $T^{(i)}(\boldsymbol{\rho}, L) = U_{\text{turb}}^{(i)}$, with $U_{\text{turb}}^{(i)}$ the unitary operator for a particular realization i of turbulence fluctuations. Thereby, the propagated field $u(\boldsymbol{\rho}, L)$ is spread over the entire receiver plane at $z = L$. In practice, the radiation field in the transmitter and receiver

planes is confined by finite-size apertures, resulting in a violation of unitarity, due to the geometric truncation of the input and output beams described by the projectors Π_T and Π_R. Henceforth, unless stated otherwise, by the turbulence operator we therefore understand a realistic scenario with finite-size circular apertures,[19,40] such that $T^{(i)}(\boldsymbol{\rho}, L) = \Pi_R\, U^{(i)}_{\rm turb}\, \Pi_T$.

2.4 Construction of the turbulence transmission matrix

The *transmission matrix* of turbulence $t^{(i)}(\boldsymbol{\rho}, L)$ is a representation of the turbulence operator $T^{(i)}(\boldsymbol{\rho}, L)$ in a particular basis. $t^{(i)}(\boldsymbol{\rho}, L)$ maps S input basis modes $\{|\phi_s\rangle\}$ $(1 \le s \le S)$ into Q output basis modes $\{|\psi_q\rangle\}$ $(1 \le q \le Q)$,

$$|\psi_q\rangle = \sum_{s=1}^{S} t^{(i)}_{qs}(\boldsymbol{\rho}, L)|\phi_s\rangle, \tag{6}$$

with $t^{(i)}_{qs}(\boldsymbol{\rho}, L) = \langle\psi_q|T^{(i)}(\boldsymbol{\rho}, L)|\phi_s\rangle$.

As the input basis, we choose Laguerre-Gaussian (LG) modes. This choice is suggested by the cylindrical symmetry of the problem and by the actual quantum communication protocols relying on OAM encoding.[15,18,19,31,41] Furthermore, in absence of turbulence as well as under weak turbulence conditions characterized by negligible scintillations ($\sigma_R^2 \ll 1$), the transmitting and receiving eigenmodes of the free-space channel are given by prolate spheroidal wavefunctions,[24,27] which are closely related to LG modes.[25]

The number S is estimated given the transmitter aperture diameter $D_T = 14.43\,\text{cm}$ and the width of fundamental mode $w_0 = 1.0\,\text{cm}^{\dagger}$. Recalling that for LG modes, the beam width increases with the azimuthal and radial indices, l and p, respectively, as[13] $w \approx w_0\sqrt{2p + |l| + 1}$, we ensure that $w < D_T$ (otherwise, geometric beam truncation leads to power and entanglement losses[43]). The latter inequality is well satisfied by setting $p \le 20$, $|l| \le 20$, wherefrom we obtain $S = 861$.

As for the output basis, we employ the pixel basis, for which Q is the number of pixels within the receiving aperture with diameter $D_R = 57.81$ cm‡. We take a standard grid of 512×512 pixels[28] to represent a square $A = 80 \times 80\,\text{cm}^2$. Hence, $Q \simeq \pi(512 \times D_R)^2/\,(4A) \approx 107500$.

2.5 Eigenmodes of light in turbulence

To identify highly transmitting modes of light in turbulence, we perform a *singular value decomposition* (SVD)[23,32] of the transmission matrix,

$$t^{(i)}(\boldsymbol{\rho}, L) = U D_{\rm diag} V^{\dagger}, \tag{7}$$

where $D_{\rm diag} = \text{diag}(\tau_1, \ldots, \tau_S)$ is a $Q \times S$ diagonal matrix whose elements are the *singular values* τ_k of the transmission matrix, which can be calculated as the square roots of the eigenvalues of the Hermitian matrix $t^{(i)\dagger}(\boldsymbol{\rho}, L)t^{(i)}(\boldsymbol{\rho}, L)$; U and V have dimensions $Q \times Q$ and $S \times S$ and $U^{\dagger}U = \mathbf{I}$, $V^{\dagger}V = \mathbf{I}$; the columns of the matrices U and V are the *singular vectors* $|u_k\rangle = \sum_{q=1}^{Q} u_{kq}|\psi_q\rangle$ and $|v_k\rangle = \sum_{s=1}^{S} v_{ks}|\phi_s\rangle$, respectively. SVD (7) amounts to the following representation of the transmission matrix:

$$t^{(i)}(\boldsymbol{\rho}, L) = \sum_{s=1}^{S} \tau_s |u_s\rangle\langle v_s|. \tag{8}$$

Next, we present our results for the singular values and the spatial distribution of the highly transmitting modes under different turbulence conditions.

---

†The chosen values of D_T and w_0 are approximately equal to the experimental ones.[42]

‡While the size of the transmitter aperture allows to avoid geometric truncation of all modes from the input basis, the increased size of the receiver aperture does so for diffracted output modes.

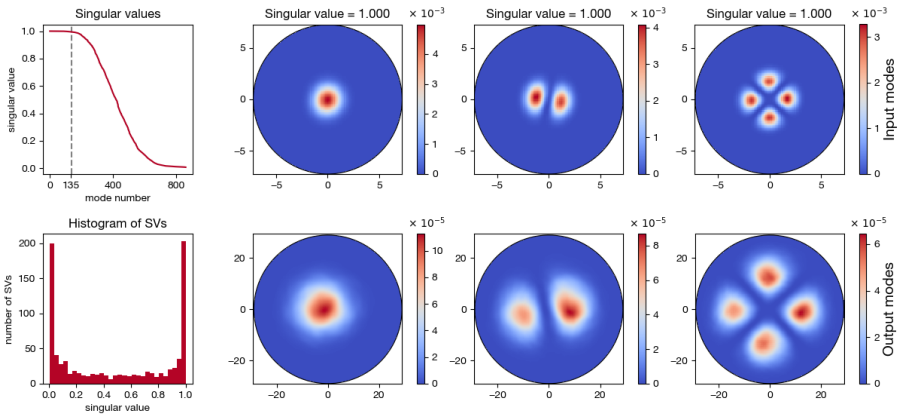

$(a) \quad \sigma_{\mathrm{R}}^2 = 0.02$

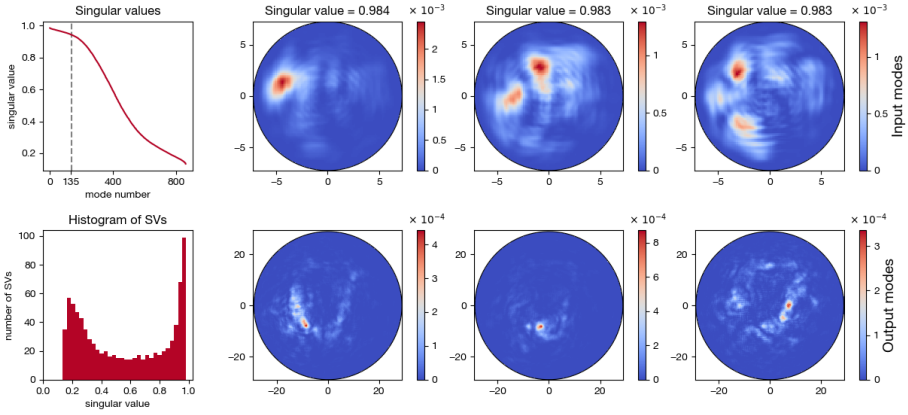

$(b) \quad \sigma_{\mathrm{R}}^2 = 2.48$

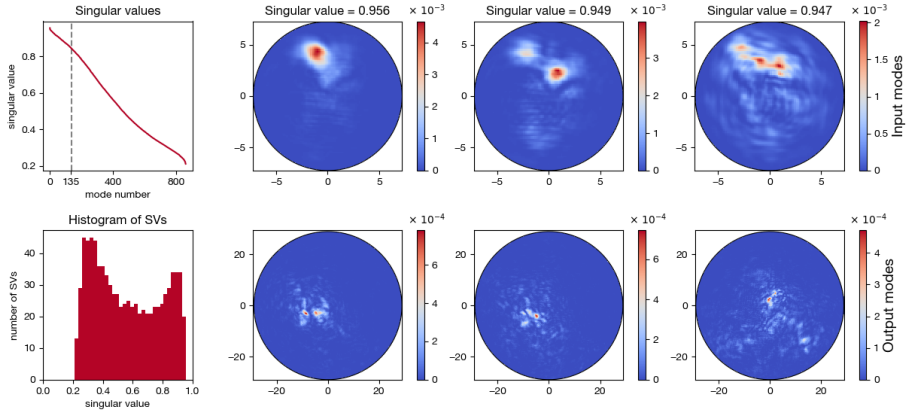

$(c) \quad \sigma_{\mathrm{R}}^2 = 6.31$

Figure 1. Distributions of singular values as a function of the mode number together with the corresponding histograms underneath (left column), and intensity distributions of three singular vectors $|v_s\rangle$ (input modes: odd row numbers) and their associated singular vectors $|u_s\rangle$ (output modes, even row numbers) with highest singular values (given above the input modes), for three values of Rytov variance σ_R^2: (a) 0.02, (b) 2.48, (c) 6.31. Note the different labels of the x and y axes of the input and output modes, reflecting the different diameters of the transmitter and receiver apertures (14.43 cm and 57.81 cm, respectively).

3. RESULTS

We consider the propagation of a monochromatic wave with wavelength $\lambda = 1064\,\mathrm{nm}$ and width $w_0 = 1.0\,\mathrm{cm}$ across a horizontal free-space link of length $L = 6000\,\mathrm{m}$. As already mentioned, a turbulent medium is confined by two circular apertures with diameters $D_T = 14.43\,\mathrm{cm}$ and $D_R = 57.81\,\mathrm{cm}$ in the transmitter and receiver planes, respectively. In absence of turbulence, such free-space link supports[24,25]

$$M = \frac{\pi D_R^2}{4(\lambda L/D_T)^2} \approx 135 \tag{9}$$

highly transmitting modes. We calculated eigenmodes for three values of the turbulence strength strength, $W = 0.02,\ 0.28,\ 0.50$, corresponding to weak ($\sigma_R^2 = 0.02$), moderate ($\sigma_R^2 = 2.48$), and strong ($\sigma_R^2 = 6.31$) scintillation, respectively. The associated transmission matrices were generated using 1, 9 and 23 phase screens. SVD of the transmission matrix, according to (7), renders the representations (8) in terms of singular values τ_s and left and right singular vectors $|v_s\rangle$ and $|u_s\rangle$. The results of this analysis are displayed in Fig. 1.

We observe that under weak scintillation ($\sigma_R^2 = 0.02$), there are 134 highly transmitting modes with $\tau_s \geq 0.995$, which is close to the theoretical value in absence of turbulence,[24,25] $M = 135$ (see Eq. (9) and the vertical dashed line in the top left panel of Fig. 1). It is under these conditions that a similarity of eigenmodes with $\tau_s \approx 1$ to LG modes was shown.[25] To illustrate their typical behaviour, we here provide intensity distributions for three such modes. Both the input and output modes in this case exhibit intensity distributions indeed reminiscent of LG modes with $p = 0$, $l = 0$ (second column, first and second row) or of superpositions of the LG modes $p = 0$, $l = \pm 1$ (third column, first and second row) and of the LG modes $p = 0$, $l = \pm 2$ (fourth column, first and second row) with two and four lobes, respectively (see, e.g.[41]). Despite the very small value of the Rytov variance, the combined impact of turbulence distortions and diffraction is manifest in slight deviations of the intensity distributions of the input and output modes from the intensity distributions of LG modes and superpositions thereof.

As the Rytov variance increases to $\sigma_R^2 = 2.48$ and $\sigma_R^2 = 6.31$, we observe that the singular value histograms (Fig. 1, left column, rows four and six) rapidly lose the bi-modal shape of the weak turbulence limit and flatten out. Still there are more than 100 modes with $\tau_s > 0.95$ (moderate scintillation) and $\tau_s > 0.87$ (strong scintillation). The input and output singular vectors corresponding to large singular values have intensity distributions that, at first glance, look random (see rows three to six in Fig. 1). However, in all cases most of the intensity distribution is *localized* at random positions in the tranverse input and output planes around one, sometimes two, maxima with a characteristic width of the order of $\sim 1\,\mathrm{cm} = w_0$. These maxima resemble the displaced intensity distributions of the basis modes garnished by noise. The structure and transverse localization properties of these spatial modes will be explored in future work.

4. CONCLUSION

We studied spatial eigenmodes of light in frozen atmospheric turbulence. We considered a horizontal channel wherein a turbulent medium is confined between two finite-size circular apertures. To describe monochromatic wave propagation across this channel, we employed multiple phase screens method and generated channel's transmission matrix for weak, moderate, and strong scintillation conditions. By means of the singular value decomposition of the transmission matrix, even within the strong scintillation regime, we identified ~ 100 highly transmitting eigenmodes in the transmitter and receiver planes that are mapped onto each other with little loss. Under weak scintillation, our calculations confirm the previous results[25,26] that eigenmodes with large singular values are closely related to Laguerre-Gaussian modes. However, under moderate to strong scintillation, the highly transmitting eigenmodes differ very significantly from standard mode families, and are characterized by pronounced transverse localization. These promising observations, and their consequences for high-dimensional spatial encoding in atmospheric turbulence deserve further studies.

Acknowledgements

V.S. acknowledges support by the Strategiefonds der Albert-Ludwigs-Universität Freiburg.

REFERENCES

[1] N. Gisin and R. Thew, "Quantum communication," *Nat. Photon.* **1**, pp. 165–171, 2007.

[2] R. Ursin, F. Tiefenbacher, T. Schmitt-Manderbach, H. Weier, T. Scheidl, M. Lindenthal, B. Blauensteiner, T. Jennewein, J. Perdigues, P. Trojek, B. Omer, M. Furst, M. Meyenburg, J. Rarity, Z. Sodnik, C. Barbieri, H. Weinfurter, and A. Zeilinger, "Entanglement-based quantum communication over 144 km," *Nat. Phys.* **3**, pp. 481–486, 2007.

[3] S.-K. Liao, W.-Q. Cai, J. Handsteiner, B. Liu, J. Yin, L. Zhang, D. Rauch, M. Fink, J.-G. Ren, W.-Y. Liu, Y. Li, Q. Shen, Y. Cao, F.-Z. Li, J.-F. Wang, Y.-M. Huang, L. Deng, T. Xi, L. Ma, T. Hu, L. Li, N.-L. Liu, F. Koidl, P. Wang, Y.-A. Chen, X.-B. Wang, M. Steindorfer, G. Kirchner, C.-Y. Lu, R. Shu, R. Ursin, T. Scheidl, C.-Z. Peng, J.-Y. Wang, A. Zeilinger, and J.-W. Pan, "Satellite-relayed intercontinental quantum network," *Phys. Rev. Lett.* **120**, p. 030501, 2018.

[4] A. Forbes and I. Nape, "Quantum mechanics with patterns of light: Progress in high dimensional and multidimensional entanglement with structured light," *AVS Quantum Science* **1**, p. 011701, 2019.

[5] N. J. Cerf, M. Bourennane, A. Karlsson, and N. Gisin, "Security of quantum key distribution using d-level systems," *Phys. Rev. Lett.* **88**, p. 127902, 2002.

[6] A. C. Dada, J. Leach, G. S. Buller, M. J. Padgett, and E. Andersson, "Experimental high-dimensional two-photon entanglement and violations of generalized bell inequalities," *Nat. Phys.* **7**, pp. 677–680, 2011.

[7] M. Padgett, J. Courtial, and L. Allen, "Light's orbital angular momentum," *Physics Today* **57**, pp. 35–40, 2004.

[8] L. Allen, M. W. Beijersbergen, R. J. C. Spreeuw, and J. P. Woerdman, "Orbital angular momentum of light and the transformation of laguerre-gaussian laser modes," *Phys. Rev. A* **45**, pp. 8185–8189, 1992.

[9] F. Gori, G. Guattari, and C. Padovani, "Bessel-Gauss beams," *Opt. Commun.* **64**, pp. 491 – 495, 1987.

[10] M. A. Cox, L. Maqondo, R. Kara, G. Milione, L. Cheng, and A. Forbes, "The resilience of Hermite– and Laguerre–Gaussian modes in turbulence," *J. Lightwave Technol.* **37**, pp. 3911–3917, 2019.

[11] X. Gu, L. Chen, and M. Krenn, "Phenomenology of complex structured light in turbulent air," *Opt. Express* **28**, pp. 11033–11050, 2020.

[12] M. A. Cox, N. Mphuthi, I. Nape, N. P. Mashaba, L. Cheng, and A. Forbes, "Structured light in turbulence," *Prieprint arXiv:2005.14586v1* , 2020.

[13] L. C. Andrews and R. L. Phillips, *Laser Beam Propagation through Random Media*, SPIE Press, Bellingham, Second ed., 2005.

[14] J. A. Anguita, M. A. Neifeld, and B. V. Vasic, "Turbulence-induced channel crosstalk in an orbital angular momentum-multiplexed free-space optical link," *Appl. Opt.* **47**, pp. 2414–2429, 2008.

[15] M. Krenn, J. Handsteiner, M. Fink, R. Fickler, and A. Zeilinger, "Twisted photon entanglement through turbulent air across Vienna," *PNAS* **46**, p. 14197, 2015.

[16] A. Sit, F. Bouchard, R. Fickler, J. Gagnon-Bischoff, H. Larocque, K. Heshami, D. Elser, C. Peuntinger, K. Günthner, B. Heim, C. Marquardt, G. Leuchs, R. W. Boyd, and E. Karimi, "High-dimensional intracity quantum cryptography with structured photons," *Optica* **4**, pp. 1006–1010, 2017.

[17] M. A. Cox, L. Cheng, C. Rosales-Guzmán, and A. Forbes, "Modal diversity for robust free-space optical communications," *Phys. Rev. Applied* **10**, p. 024020, 2018.

[18] B. Ndagano and A. Forbes, "Characterization and mitigation of information loss in a six-state quantum-key-distribution protocol with spatial modes of light through turbulence," *Phys. Rev. A* **98**, p. 062330, 2018.

[19] G. Sorelli, N. Leonhard, V. N. Shatokhin, C. Reinlein, and A. Buchleitner, "Entanglement protection of high-dimensional states by adaptive optics," *New J. Phys.* **21**, p. 023003, 2019.

[20] J. Zhao, Y. Zhou, B. Braverman, C. Liu, K. Pang, N. K. Steinhoff, G. A. Tyler, A. E. Willner, and R. W. Boyd, "Performance of real-time adaptive optics compensation in a turbulent channel with high-dimensional spatial-mode encoding," *Opt. Express* **28**, pp. 15376–15391, 2020.

[21] C. M. Mabena and F. S. Roux, "Quantum channel correction with twisted light using compressive sensing," *Phys. Rev. A* **101**, p. 013807, 2020.

[22] N. Zhao, X. Li, G. Li, and J. M. Kahn, "Capacity limits of spatially multiplexed free-space communication," *Nat. Photon.* **9**, pp. 822–826, 2015.

[23] S. Rotter and S. Gigan, "Light fields in complex media: Mesoscopic scattering meets wave control," *Rev. Mod. Phys.* **89**, p. 015005, 2017.

[24] J. H. Shapiro, "Normal-mode approach to wave propagation in the turbulent atmosphere," *Appl. Opt.* **13**, pp. 2614–2619, 1974.

[25] L. Borcea, J. Garnier, and K. Sølna, "Multimode communication through the turbulent atmosphere," *J. Opt. Soc. Am. A* **37**, pp. 720–730, 2020.

[26] A. Belmonte and J. M. Kahn, "Approaching fundamental limits to free-space communication through atmospheric turbulence," *Proc. SPIE* **10559**, pp. 70 – 76, 2018.

[27] D. Slepian, "Prolate spheroidal wave functions, Fourier analysis and uncertainty — IV: Extensions to many dimensions; generalized prolate spheroidal functions," *Bell Sys. Tech. J.* **43**, pp. 3009–3057, 1964.

[28] J. D. Schmidt, *Numerical Simulation of Optical Wave Propagtion*, SPIE Press, Bellingham, 2010.

[29] J. M. Martin and S. M. Flatté, "Intensity images and statistics from numerical simulation of wave propagation in 3-d random media," *Appl. Opt.* **27**, pp. 2111–2126, 1988.

[30] R. G. Lane, A. Glindemann, and J. C. Dainty, "Simulation of a Kolmogorov phase screen," *Waves Rand. Media* **2**, pp. 209–224, 1992.

[31] N. Leonhard, G. Sorelli, V. N. Shatokhin, C. Reinlein, and A. Buchleitner, "Protecting the entanglement of twisted photons by adaptive optics," *Phys. Rev. A* **97**, p. 012321, 2018.

[32] D. A. B. Miller, "Waves, modes, communications, and optics: a tutorial," *Adv. Opt. Photon.* **11**, pp. 679–825, 2019.

[33] R. Tyson, *Principles of Adaptive Optics*, CRC Press, Boca Raton, 2010.

[34] V. I. Tatarskii, "Light propagation in a medium with random refractive index inhomogeneities in the Markov random process approximation," *Sov. Phys. JETP* **29**, pp. 1133–1138, 1969.

[35] A. N. Kolmogorov, "The local structure of turbulence in incompressible viscous fluid for very large Reynolds numbers," *Dokl. Acad. Nauk SSSR* **30**, p. 4, 1941.

[36] C. Paterson, "Atmospheric turbulence and orbital angular momentum of single photons for optical communication," *Phys. Rev. Lett.* **94**, p. 153901, 2005.

[37] V. P. Lukin and B. V. Fortes, *Adaptive Beaming and Imaging in the Turbulent Atmosphere*, SPIE Press, Bellingham, 2002.

[38] T. Eichhorn, "*Transport of High-Dimensional Photonic States across a Turbulent Atmosphere*," Master's Thesis (Albert-Ludwigs-Universität Freiburg, 2018).

[39] G. Sorelli, "*Quantum state transfer in diffractive and refractive media*," Dissertation (Albert-Ludwigs-Universität Freiburg, 2019).

[40] J. Schuler, "*Spatial eigenmodes of atmospheric turbulence*," Bachelor's thesis (Albert-Ludwigs-Universität Freiburg, 2018).

[41] M. Krenn, J. Handsteiner, M. Fink, R. Fickler, R. Ursin, M. Malik, and A. Zeilinger, "Twisted light transmission over 143 km," *PNAS* **113**, p. 13648, 2016.

[42] M. P. J. Lavery, C. Peuntinger, K. Günthner, P. Banzer, D. Elser, R. W. Boyd, M. J. Padgett, C. Marquardt, and G. Leuchs, "Free-space propagation of high-dimensional structured optical fields in an urban environment," *Sci. Adv.* **3**(10), p. e1700552, 2017.

[43] G. Sorelli, V. N. Shatokhin, F. S. Roux, and A. Buchleitner, "Entanglement of truncated quantum states," *Quantum Sci. Technol.* **5**, p. 035012, 2020.